

Two New $\mu - \tau$ Deviated Neutrino Mass Matrix Textures

Pralay Chakraborty*

Physics Department, Gauhati University, India

Tanmay Dev†

Physics Department, Gauhati University, India

Subhankar Roy‡

Physics Department, Gauhati University, India.

(Dated: April 23, 2024)

arXiv:2404.14264v1 [hep-ph] 22 Apr 2024

Abstract

We propose two new neutrino mass matrix textures deviating from $\mu - \tau$ symmetry and explore their phenomenological implications. Both textures predict θ_{23} and δ within sharp bounds while considering both normal and inverted ordering of neutrino masses. We try to realize these proposed textures within the framework of the seesaw mechanism, in association with the $SU(2)_L \times A_4 \times Z_3$ symmetry group.

I. INTRODUCTION

In the year 1957, Bruno Pontecorvo proposed the idea of neutrino oscillation, suggesting that neutrinos change their identity as they move through space [1]. This phenomenon arises from the fact that the three flavours of neutrinos ($\nu_{l=e,\mu,\tau}$) are admixtures of three mass eigenstates ($\nu_{i=1,2,3}$) with corresponding mass values ($m_{i=1,2,3}$). The phenomenon of neutrino oscillation predicts that neutrinos must have non-zero mass, which contradicts with the predictions of the Standard Model (SM) [2–4]. To understand the origin of neutrino mass, it is necessary to explore theories that go beyond the SM. The neutrino mass matrix (M_ν) originates from the Yukawa Lagrangian, formulated within the framework of the see-saw mechanism [5–7]. The M_ν contains twelve parameters: three mass eigenvalues ($m_{i=1,2,3}$), three mixing angles ($\theta_{12}, \theta_{13}, \theta_{23}$), three CP phases (δ, α, β), and three unphysical phases (ϕ_1, ϕ_2, ϕ_3). In the literature, various constraints, such as texture zeroes [8], vanishing minors [9], hybrid textures [10] and $\mu - \tau$ symmetry [11, 12] have been applied to M_ν so that some physical parameters can be predicted. It is worth noting that experiments have ruled out the $\mu - \tau$ symmetry due to its prediction of θ_{13} being zero. Despite this, the $\mu - \tau$ symmetry along with its predictions has been well-established, the theorists have made several attempts to explore deviations from the exact $\mu - \tau$ symmetry, in the form of $\mu - \tau$ anti-symmetry [13], $\mu - \tau$ reflection symmetry [14], $\mu - \tau$ mixed symmetry [15, 16], etc. In that light, we propose two new $\mu - \tau$ deviated neutrino mass matrix textures as shown in the following,

* pralay@gauhati.ac.in

† tanmaydev177@gmail.com

‡ subhankar@gauhati.ac.in

$$M_\nu^1 = \begin{bmatrix} A & -B & -iB/2 \\ -B & B & D \\ -iB/2 & D & 2B \end{bmatrix}, \quad (1)$$

$$M_\nu^2 = \begin{bmatrix} A & B & (iB)^* \\ B & 2B^* & D \\ (iB)^* & D & -2B \end{bmatrix}, \quad (2)$$

where, A , B and D appearing in both the textures are complex parameters.

The plan of the paper is outlined as follows: In section (II), we give the formalism of our work. The section (III) is devoted to the numerical analysis and possible symmetry realization. In section (IV), we conclude.

II. FORMALISM

In addition to M_ν , the neutrino physics phenomenology deals with an important quantity known as the Pontecorvo-Maki-Nakagawa-Sakata (PMNS) matrix [17], V , which is a 3×3 unitary matrix. In general, the PMNS matrix is defined in a basis where the charged lepton mass matrix is diagonal (flavour basis). The Particle Data Group has adopted a parametrization scheme for V as shown in the following,

$$V = P_\phi \cdot U \cdot P_M, \quad (3)$$

where, $P_\phi = \text{diag}(e^{i\phi_1}, e^{i\phi_2}, e^{i\phi_3})$ and $P_M = \text{diag}(e^{i\alpha}, e^{i\beta}, 1)$. The matrix U is depicted as shown below,

$$U = \begin{bmatrix} 1 & 0 & 0 \\ 0 & c_{23} & s_{23} \\ 0 & -s_{23} & c_{23} \end{bmatrix} \times \begin{bmatrix} c_{13} & 0 & s_{13} e^{-i\delta} \\ 0 & 1 & 0 \\ -s_{13} e^{i\delta} & 0 & c_{13} \end{bmatrix} \times \begin{bmatrix} c_{12} & s_{12} & 0 \\ -s_{12} & c_{12} & 0 \\ 0 & 0 & 1 \end{bmatrix}, \quad (4)$$

where, $s_{ij} = \sin \theta_{ij}$ and $c_{ij} = \cos \theta_{ij}$.

As discussed in Section I, M_ν shelters information about all physical parameters. To extract this information, we need to diagonalize M_ν : $M^d = V^T M_\nu V$. It is to be noted that

the unphysical phases ($\phi_{i=1,2,3}$) can be removed from V by redefining the charged lepton fields in terms of these phases. However, in the present work, we stick to the general form of M_ν containing the unphysical phases. We distinguish M_ν from \tilde{M}_ν that excludes the unphysical phases as shown in the following,

$$M_\nu = P_\phi^* \tilde{M}_\nu P_\phi^*, \quad (5)$$

where P_ϕ carries the unphysical phases.

The constrained relations appearing in M_ν^1 as shown in Eq. (1) hold good provided the following conditions for the unphysical phases are satisfied,

$$\phi_2 - \phi_3 = \text{Arg}[(\tilde{M}_\nu^1)_{12}] - \text{Arg}[(\tilde{M}_\nu^1)_{13}] + \frac{\pi}{2}, \quad (6)$$

$$\phi_2 - \phi_3 = \frac{1}{2} \left(\text{Arg}[(\tilde{M}_\nu^1)_{22}] - \text{Arg}[(\tilde{M}_\nu^1)_{33}] \right), \quad (7)$$

$$\phi_1 - \phi_2 = \text{Arg}[(\tilde{M}_\nu^1)_{12}] - \text{Arg}[(\tilde{M}_\nu^1)_{22}] - \frac{\pi}{2}. \quad (8)$$

On the other hand, for M_ν^2 as appearing in Eq. (2), the conditions for the unphysical phases are given by,

$$2\phi_1 + \phi_2 + \phi_3 = \text{Arg}[(\tilde{M}_\nu^2)_{12}] + \text{Arg}[(\tilde{M}_\nu^2)_{13}] + \frac{\pi}{2}, \quad (9)$$

$$\phi_2 + \phi_3 = \frac{1}{2} \left(\text{Arg}[(\tilde{M}_\nu^2)_{22}] + \text{Arg}[(\tilde{M}_\nu^2)_{33}] - \frac{\pi}{2} \right), \quad (10)$$

$$\phi_1 + \phi_2 - 2\phi_3 = \text{Arg}[(\tilde{M}_\nu^2)_{12}] - \text{Arg}[(\tilde{M}_\nu^2)_{33}] - \frac{\pi}{2}. \quad (11)$$

It is to be noted that the choice between sticking to M_ν or \tilde{M}_ν is subjective. However, keeping the said phases intact in M_ν provides some phenomenological prospects. The importance of these unphysical phases is highlighted in the Ref. [14]. It is evident from Eq. (5) that \tilde{M}_ν does not involve the unphysical phases. In this regard, constraints applied to \tilde{M}_ν ensure that predictions of physical parameters remain unaffected by these phases. However, the same is not true if we are dealing with M_ν . In most studies, model builders prefer to stick to \tilde{M}_ν , along with the fact that ϕ_1 , ϕ_2 , and ϕ_3 are removed by redefining the charged lepton fields. However, there are no such theoretical impositions that actually dictate the removal of the said phases. In the present work, we try to formulate constraints on the mass matrix elements of M_ν rather than \tilde{M}_ν .

III. PROPOSED TEXTURE VIABILITY

In this section, we discuss the phenomenological implications of the proposed textures M_ν^1 and M_ν^2 in the light of experimental observations. In addition, we shall try to realize the proposed textures from group theoretical framework.

A. Numerical analysis

The proposed texture M_ν^1 deals with three constrained relations as shown in the following,

$$(M_\nu^1)_{12} = 2i(M_\nu^1)_{13}, \quad (12)$$

$$(M_\nu^1)_{22} = \frac{(M_\nu^1)_{33}}{2}, \quad (13)$$

$$(M_\nu^1)_{22} = -(M_\nu^1)_{12}. \quad (14)$$

The fourth relation $(M_\nu^1)_{33} = -2(M_\nu^1)_{12}$ is not independent and can be derived from the above three.

The equations arising in (12) and (14) are complex equations and give rise to six real equations as shown in the following,

$$\text{Re}[(M_\nu^1)_{12}] + 2 \text{Im}[(M_\nu^1)_{13}] = 0, \quad (15)$$

$$\text{Im}[(M_\nu^1)_{12}] - 2 \text{Re}[(M_\nu^1)_{13}] = 0, \quad (16)$$

$$\text{Re}[(M_\nu^1)_{22}] - \frac{1}{2} \text{Re}[(M_\nu^1)_{33}] = 0, \quad (17)$$

$$\text{Im}[(M_\nu^1)_{22}] - \frac{1}{2} \text{Im}[(M_\nu^1)_{33}] = 0, \quad (18)$$

$$\text{Im}[(M_\nu^1)_{22}] + \text{Re}[(M_\nu^1)_{12}] = 0, \quad (19)$$

$$\text{Im}[(M_\nu^1)_{22}] + \text{Im}[(M_\nu^1)_{12}] = 0. \quad (20)$$

Needless to mention, the left hand side of above six equations involves twelve parameters including the unphysical phases. We solve the Eqs. (15)-(20) numerically and generate the sufficient number of random numbers for the parameters Δm_{21}^2 , Δm_{31}^2 , θ_{12} , θ_{13} , θ_{23} and δ and obtain the correlations plots. For normal ordering, we observe that θ_{23} lies in the lower octant and takes minimum and maximum values as 41.83° and 42.19° whereas the bound

for δ is constrained to take the minimum and maximum values as 217.24° and 221.86° respectively (see Figs. 1(a)-1(c)). For Inverted ordering, it is seen that θ_{23} lies in the upper octant with minimum and maximum values as 49.34° and 49.54° whereas δ is constrained to a sharp bound with minimum value 308.07° and maximum value 315.42° respectively (see Figs. 2(a)-2(c)). In addition to this, the obtained bound for the mass squared differences (Δm_{21}^2 and Δm_{31}^2) and two mixing angles (θ_{12} and θ_{13}), considering the normal orderings are consistent with the experimental observations [18, 19]. On the other hand, the mixing scheme obtained for inverted ordering aligns well with experimental observations except for θ_{13} (see Fig. 2(b)). Hence, for inverted ordering, the texture M_ν^1 is ruled out in the light of experimental evidences. For the above analysis, the choice of input parameters are taken as per Table I (for normal ordering) and Table II (for inverted ordering).

The texture M_ν^2 shelters three constrained relations as shown below,

$$(M_\nu^2)_{12} = (i(M_\nu^2)_{13})^*, \quad (21)$$

$$(M_\nu^2)_{22} = -((M_\nu^2)_{33})^*, \quad (22)$$

$$(M_\nu^2)_{33} = -2((M_\nu^2)_{12}). \quad (23)$$

For M_ν^2 as well, there is a corresponding dependent relation: $(M_\nu^1)_{22} = 2(M_\nu^1)_{12}^*$. This relation can be derived from the aforementioned three relations.

As before, the three complex relations appearing in Eqs.(21) and (23) give rise to six real equations as shown below,

$$\text{Re}[(M_\nu^2)_{12}] + \text{Im}[(M_\nu^2)_{13}] = 0, \quad (24)$$

$$\text{Im}[(M_\nu^2)_{12}] + \text{Re}[(M_\nu^2)_{13}] = 0, \quad (25)$$

$$\text{Re}[(M_\nu^2)_{22}] + \text{Re}[(M_\nu^2)_{33}] = 0, \quad (26)$$

$$\text{Im}[(M_\nu^2)_{22}] - \text{Im}[(M_\nu^2)_{33}] = 0, \quad (27)$$

$$\text{Re}[(M_\nu^2)_{33}] + 2 \text{Re}[(M_\nu^2)_{12}] = 0, \quad (28)$$

$$\text{Im}[(M_\nu^2)_{33}] + 2 \text{Im}[(M_\nu^2)_{12}] = 0. \quad (29)$$

Following the similar analysis, we generate the correlations plots for the parameters Δm_{21}^2 , Δm_{31}^2 , θ_{12} , θ_{13} , θ_{23} and δ , considering both normal and inverted orderings. It is evident

from the graphical visualization that for normal ordering, θ_{23} lies in the lower octant with minimum value 44.87° and maximum value 44.89° respectively. A constrained bound for δ is obtained with minimum and maximum value as 174.77° and 179.28° respectively (see Figs. 3(a)-3(c)). For inverted ordering, it is found that θ_{23} lies in the lower octant and takes the minimum and maximum value as 44.77° and 44.98° while δ is constrained to a sharp bound with minimum value 336.87° and maximum value 340.93° respectively (see Figs. 4(a)-4(c)). In addition, the prediction of the mass squared differences and mixing angles obtained for both the orderings are consistent with experimental data [18, 19]. The choice of the input parameters are listed in Table III (normal ordering) and Table IV (inverted ordering). We highlight that in the present work, the sum of three neutrino masses is consistent with cosmological data i.e., $\leq 0.12 eV$ [20].

The justification of the Majorana nature of neutrinos is subjected to the discovery of neutrinoless double beta decay [21, 22]. The effective Majorana neutrino mass, denoted as $m_{\beta\beta} = |\sum_{k=1}^3 U_{1k}^2 m_k|$, is a observational parameter in neutrinoless double beta decay, where, m_1 , m_2 and m_3 are the three mass eigenvalues, U_{11}, U_{12} and U_{13} are the elements of the PMNS matrix that carry the information of the Majorana phases. In recent years, several experiments have provided the upper bounds of $m_{\beta\beta}$: SuperNEMO(Se^{82}) as $67 - 131$ meV, GERDA(Ge^{76}) as $104 - 228$ meV, EXO-200(Xe^{136}) as $111 - 477$ meV, CUORE(Te^{130}) as $75 - 350$ meV and KamLAND-Zen(Xe^{136}) as $61 - 165$ meV [23–30]. In this regard, we predict the parameter $m_{\beta\beta}$ from the proposed textures (see Figs. 5(a)-5(b)), in the light of both normal and inverted orderings.

B. Texture Feasibility from Symmetry

To understand the proposed texture from symmetry framework, we try to incorporate see-saw mechanism in association with A_4 group. In this regard, we extend the field content of the SM by introducing three right-handed neutrinos ($\nu_{eR}, \nu_{\mu R}, \nu_{\tau R}$), a scalar singlet (ζ), and two scalar triplets (ϕ, Δ). The transformation properties of the field content are summarised in Table V. The $SU(2)_L \times A_4 \times Z_3$ invariant Lagrangian is constructed in the following way,

$$\begin{aligned}
-\mathcal{L}_Y &= y_e(\bar{D}_{l_L}H)_1 e_{R_1} + y_\mu(\bar{D}_{l_L}H)_{1'} \mu_{R_1''} + y_\tau(\bar{D}_{l_L}H)_{1''} \tau_{R_1'} + y_1(\bar{D}_{l_L}\Phi)_1 \nu_{eR_1} \\
&+ y_2(\bar{D}_{l_L}\Phi)_{1''} \nu_{\mu R_1'} + y_3(\bar{D}_{l_L}\Phi)_{1'} \nu_{\tau 1''} + \frac{1}{2}y_{R_1}(\bar{\nu}^c_{e_R} \nu_{e_R})_1 \zeta + \frac{1}{2}y_{R_2} \\
&[(\bar{\nu}^c_{\mu_R} \nu_{\tau_R}) + (\bar{\nu}^c_{\tau_R} \nu_{\mu_R})] \zeta + y_{T_2}(\bar{D}_{l_L}D_{l_L}^c)_{3_S} \Delta_3 + h.c.
\end{aligned} \tag{30}$$

The additional group Z_3 is incorporated to cut short some undesired terms. The vacuum expectation values (vev) for the scalar fields are chosen as: $\langle H \rangle_0 = v_H(1, 1, 1)^T$ and $\langle \Phi \rangle_0 = v_\Phi(1, 1, 1)^T$, $\langle \zeta \rangle_0 = v_\zeta$. The scalar potential in support of the chosen vacuum alignments can be found in appendix B. We derive the charged lepton mass matrix(M_L) in the following form,

$$M_L = v_H \begin{bmatrix} y_e & y_\mu & y_\tau \\ y_e & \omega y_\mu & \omega^2 y_\tau \\ y_e & \omega^2 y_\mu & \omega y_\tau \end{bmatrix}, \tag{31}$$

We diagonalize M_L as $M_L^{diag} = U_{l_L}^\dagger M_L U_{l_R}$, where $M_L^{diag} = \sqrt{3} \text{diag}(y_e, y_\mu, y_\tau)$. The U_{l_L} and U_{l_R} are expressed as,

$$U_{l_L} = \frac{1}{\sqrt{3}} \begin{bmatrix} e^{i\eta} & e^{i\kappa} & e^{i\xi} \\ e^{i\eta} & \omega e^{i\kappa} & \omega^2 e^{i\xi} \\ e^{i\eta} & \omega^2 e^{i\kappa} & \omega e^{i\xi} \end{bmatrix}, \quad U_{l_R} = \text{diag} [e^{i\eta}, e^{i\kappa}, e^{i\xi}], \tag{32}$$

The arbitrary phases η , κ and ξ in U_{l_L} and U_{l_R} are added with the motivation that the choice of eigenvectors is not unique.

The Dirac neutrino mass matrix(M_D) and the right-handed neutrino mass matrix(M_R) are obtained as shown in the following,

$$M_D = v_\Phi \begin{bmatrix} y_1 & y_2 & y_3 \\ y_1 & \omega y_2 & \omega^2 y_3 \\ y_1 & \omega^2 y_2 & \omega y_3 \end{bmatrix}, \quad M_R = \begin{bmatrix} A & 0 & 0 \\ 0 & 0 & B \\ 0 & B & 0 \end{bmatrix}, \tag{33}$$

where, $\omega = e^{2i\pi/3}$, $A = \frac{1}{2}y_{R_1}v_\zeta$ and $B = \frac{1}{2}y_{R_2}v_\zeta$.

The Type-I seesaw contribution to the neutrino mass matrix is taken as $M_{T_1} = -M_D M_R^{-1} M_D^T$. The Type-II seesaw contribution with the specific choice of vev $\langle \Delta \rangle_0 = v_\Delta(\omega^2, 0, 1)^T$ comes

as shown below,

$$M_{T_2} = y_{T_2} v_\Delta \begin{bmatrix} 0 & 1 & 0 \\ 1 & 0 & \omega^2 \\ 0 & \omega^2 & 0 \end{bmatrix}. \quad (34)$$

The neutrino mass matrix is constructed by taking the contribution from Type-I and Type-II seesaw mechanisms. Now, to move to a basis where the charged lepton mass matrix is diagonal, we incorporate a certain transformation ($U_{l_L}^T M_\nu U_{l_L}$) and obtain the effective neutrino mass matrix as shown below,

$$M_\nu^1 = \begin{bmatrix} \frac{2r}{3} - \frac{3y_1 v_\Phi^2}{2A} - \frac{3\sqrt{3}iy_1 v_\Phi^2}{2A} & -\frac{2r}{3} & \frac{ir}{3} \\ & -\frac{2r}{3} & \frac{3\sqrt{3}iy_2 y_3 v_\Phi^2}{2B} - i\left(\frac{r}{3} + \frac{3y_2 y_3 v_\Phi^2}{2B}\right) \\ & \frac{ir}{3} & \frac{3\sqrt{3}iy_2 y_3 v_\Phi^2}{2B} - i\left(\frac{r}{3} + \frac{3y_2 y_3 v_\Phi^2}{2B}\right) & \frac{4r}{3} \end{bmatrix}, \quad (35)$$

where, $r = y_{T_2} v_\Delta$. It is to be highlighted that to obtain the texture M_ν^1 , we choose $\eta = \frac{\pi}{6}$, $\kappa = \frac{3\pi}{6}$ and $\xi = \frac{2\pi}{6}$.

The proposed texture M_ν^2 can be derived from the same Lagrangian appearing in Eq. (30) under the specific choice of vev $\langle \Delta \rangle_0 = v_\Delta(0, 1, 0)^T$ and by setting $\eta = \frac{\pi}{2}$, $\kappa = \frac{\pi}{6}$ and $\xi = \frac{\pi}{3}$. We give the product rules under A_4 in appendix C.

IV. SUMMARY

To summarize, we propose two new neutrino mass matrix textures M_ν^1 and M_ν^2 deviating from $\mu - \tau$ symmetry and study their phenomenological implications. The mixing schemes provided by both textures are consistent with experimental observations. As a notable feature, both textures predict θ_{23} in the lower octant for normal ordering of neutrino masses. On the other hand, for inverted ordering, M_ν^1 predicts θ_{23} in the lower octant and M_ν^2 is ruled out in the light of experimental observations. In addition, the Dirac CP phase δ is constrained to a sharp bound. We aim to realize these proposed textures within the framework of the $SU(2)_L \times A_4 \times Z_3$ symmetry group in light of the seesaw mechanism.

As a future prospect, we aim to study the stability of the proposed textures under renormalization group running. In addition, the present work can be extended to study the baryon asymmetry based upon the proposed textures.

V. ACKNOWLEDGEMENT

The research work of PC is supported by Innovation in Science Pursuit for Inspired Research (INSPIRE), Department of Science and Technology, Government of India, New Delhi vide grant No. IF190651.

-
- [1] B. Pontecorvo, Mesonium and anti-mesonium, *Sov. Phys. JETP* 6 (1957) 429.
 - [2] S. L. Glashow, Partial Symmetries of Weak Interactions, *Nucl. Phys.* 22 (1961) 579–588. doi:10.1016/0029-5582(61)90469-2.
 - [3] S. Weinberg, A Model of Leptons, *Phys. Rev. Lett.* 19 (1967) 1264–1266. doi:10.1103/PhysRevLett.19.1264.
 - [4] M. Herrero, The Standard model, *NATO Sci. Ser. C* 534 (1999) 1–59. arXiv:hep-ph/9812242, doi:10.1007/978-94-011-4689-0_1.
 - [5] M. Yoshimura, Unified Gauge Theories and the Baryon Number of the Universe, *Phys. Rev. Lett.* 41 (1978) 281–284, [Erratum: *Phys.Rev.Lett.* 42, 746 (1979)]. doi:10.1103/PhysRevLett.41.281.
 - [6] E. K. Akhmedov, G. C. Branco, M. N. Rebelo, Seesaw mechanism and structure of neutrino mass matrix, *Phys. Lett. B* 478 (2000) 215–223. arXiv:hep-ph/9911364, doi:10.1016/S0370-2693(00)00282-3.
 - [7] R. N. Mohapatra, Seesaw mechanism and its implications, in: *SEESAW25: International Conference on the Seesaw Mechanism and the Neutrino Mass, 2004*, pp. 29–44. arXiv:hep-ph/0412379, doi:10.1142/9789812702210_0003.
 - [8] P. O. Ludl, W. Grimus, A complete survey of texture zeros in the lepton mass matrices, *JHEP* 07 (2014) 090, [Erratum: *JHEP* 10, 126 (2014)]. arXiv:1406.3546, doi:10.1007/JHEP07(2014)090.
 - [9] E. I. Lashin, N. Chamoun, One vanishing minor in the neutrino mass matrix, *Phys. Rev. D* 80 (2009) 093004. arXiv:0909.2669, doi:10.1103/PhysRevD.80.093004.
 - [10] M. Singh, Investigating the hybrid textures of neutrino mass matrix for near maximal atmospheric neutrino mixing, *Adv. High Energy Phys.* 2018 (2018) 5806743. arXiv:1803.10754, doi:10.1155/2018/5806743.

- [11] P. F. Harrison, D. H. Perkins, W. G. Scott, Tri-bimaximal mixing and the neutrino oscillation data, *Phys. Lett. B* 530 (2002) 167. [arXiv:hep-ph/0202074](#), [doi:10.1016/S0370-2693\(02\)01336-9](#).
- [12] E. Ma, Tribimaximal neutrino mixing from a supersymmetric model with A4 family symmetry, *Phys. Rev. D* 73 (2006) 057304. [arXiv:hep-ph/0511133](#), [doi:10.1103/PhysRevD.73.057304](#).
- [13] Z.-z. Xing, Z.-h. Zhao, A review of μ - τ flavor symmetry in neutrino physics, *Rept. Prog. Phys.* 79 (7) (2016) 076201. [arXiv:1512.04207](#), [doi:10.1088/0034-4885/79/7/076201](#).
- [14] Z.-z. Xing, The μ - τ reflection symmetry of Majorana neutrinos *, *Rept. Prog. Phys.* 86 (7) (2023) 076201. [arXiv:2210.11922](#), [doi:10.1088/1361-6633/acd8ce](#).
- [15] M. Dey, P. Chakraborty, S. Roy, The μ - τ mixed symmetry and neutrino mass matrix, *Phys. Lett. B* 839 (2023) 137767. [arXiv:2211.01314](#), [doi:10.1016/j.physletb.2023.137767](#).
- [16] P. Chakraborty, S. Roy, The other variants of mixed μ - τ symmetry, *Nucl. Phys. B* 992 (2023) 116252. [arXiv:2304.06737](#), [doi:10.1016/j.nuclphysb.2023.116252](#).
- [17] Z. Maki, M. Nakagawa, S. Sakata, Remarks on the unified model of elementary particles, *Prog. Theor. Phys.* 28 (1962) 870–880. [doi:10.1143/PTP.28.870](#).
- [18] I. Esteban, M. C. Gonzalez-Garcia, M. Maltoni, T. Schwetz, A. Zhou, The fate of hints: updated global analysis of three-flavor neutrino oscillations, *JHEP* 09 (2020) 178. [arXiv:2007.14792](#), [doi:10.1007/JHEP09\(2020\)178](#).
- [19] M. C. Gonzalez-Garcia, M. Maltoni, T. Schwetz, NuFIT: Three-Flavour Global Analyses of Neutrino Oscillation Experiments, *Universe* 7 (12) (2021) 459. [arXiv:2111.03086](#), [doi:10.3390/universe7120459](#).
- [20] N. Aghanim, et al., Planck 2018 results. VI. Cosmological parameters, *Astron. Astrophys.* 641 (2020) A6, [Erratum: *Astron. Astrophys.* 652, C4 (2021)]. [arXiv:1807.06209](#), [doi:10.1051/0004-6361/201833910](#).
- [21] F. Simkovic, S. M. Bilenky, A. Faessler, T. Gutsche, *Possibility of measuring the CP Majorana phases in $0\nu\beta\beta$ decay*, *Phys. Rev. D* **87** (2013) 073002.
- [22] M. J. Dolinski, A. W. P. Poon, W. Rodejohann, *Neutrinoless Double-Beta Decay: Status and Prospects*, *Ann. Rev. Nucl. Part. Sci.* **69** (2019) 219–251.
- [23] H. Ejiri, *Neutrino-mass sensitivity and nuclear matrix element for neutrinoless double beta decay*, *Universe* **6** (2020) 225.

- [24] M. Agostini, G. Benato, J. A. Detwiler, J. Menéndez, F. Vissani, Toward the discovery of matter creation with neutrinoless $\beta\beta$ decay, *Rev. Mod. Phys.* 95 (2) (2023) 025002. [arXiv:2202.01787](#), [doi:10.1103/RevModPhys.95.025002](#).
- [25] D. Q. Adams et al. Improved Limit on Neutrinoless Double-Beta Decay in ^{130}Te with CUORE. *Phys. Rev. Lett.*, 124(12):122501, 2020.
- [26] M. Agostini et al. Probing Majorana neutrinos with double- β decay. *Science*, 365:1445, 2019.
- [27] A. Gando et al. Search for Majorana Neutrinos near the Inverted Mass Hierarchy Region with KamLAND-Zen. *Phys. Rev. Lett.*, 117(8):082503, 2016. [Addendum: *Phys.Rev.Lett.* 117, 109903 (2016)].
- [28] R. Arnold, et al., *Measurement of the distribution of ^{207}Bi depositions on calibration sources for SuperNEMO*, *JINST* **16** (2021) T07012.
- [29] A. S. Barabash, et al., *Calorimeter development for the SuperNEMO double beta decay experiment*, *Nucl. Instrum. Meth. A* **868** (2017) 98?108.
- [30] D. Q. Adams, et al., *Improved Limit on Neutrinoless Double-Beta Decay in ^{130}Te with CUORE*, *Phys. Rev. Lett.* **124** (2020) 122501.

Appendix A: Tables and Figures

Parameters	Input values
m_1/eV	0.02-0.027
$\alpha/^\circ$	109-109.5
$\beta/^\circ$	266.5-267.5
$\phi_1/^\circ$	39.9-40
$\phi_2/^\circ$	0.5-1
$\phi_3/^\circ$	0.5-1

TABLE I. Numerical values of the input parameters for texture M_ν^1 (Normal Ordering)

Parameters	Input values
m_3/eV	0.012-0.015
$\alpha/^\circ$	276-276.4
$\beta/^\circ$	108.2-108.5
$\phi_1/^\circ$	74-74.4
$\phi_2/^\circ$	0.3-0.6
$\phi_3/^\circ$	0.3-0.6

TABLE II. Numerical values of the input parameters for texture M_ν^1 (Inverted Ordering)

Parameters	Input values
m_1/eV	0.022-0.027
$\alpha/^\circ$	81-81.5
$\beta/^\circ$	76-76.3
$\phi_1/^\circ$	14.5-15.5
$\phi_2/^\circ$	53.2-53.5
$\phi_3/^\circ$	17-17.2

TABLE III. Numerical values of the input parameters for texture M_ν^2 (Normal Ordering)

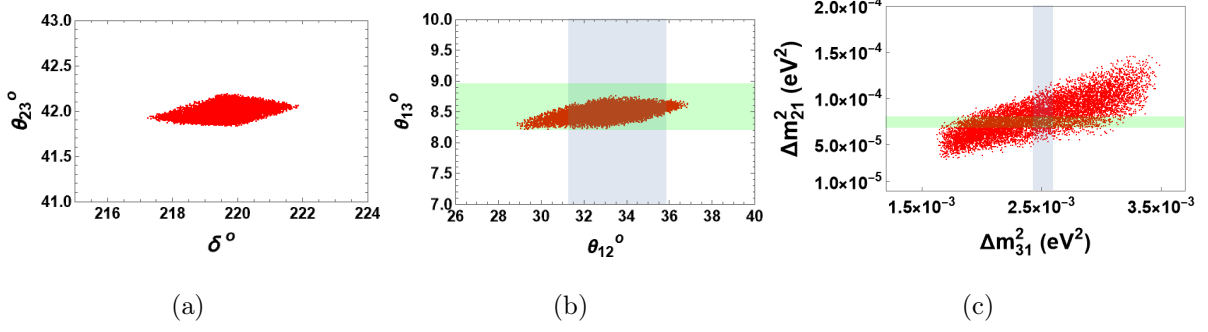


FIG. 1. The correlation plots between (a) θ_{23} and δ . (b) θ_{12} and θ_{13} . (c) Δm_{31}^2 and Δm_{21}^2 for normal ordering of neutrino masses. The blue and green strips represent the 3σ bounds for the respective parameters.

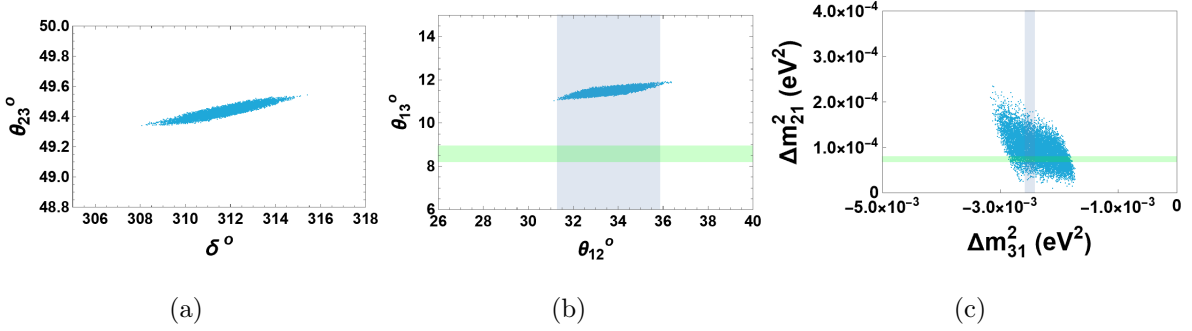


FIG. 2. The correlation plots between (a) θ_{23} and δ . (b) θ_{12} and θ_{13} . (c) Δm_{31}^2 and Δm_{21}^2 for inverted ordering of neutrino masses. The blue and green strips represent the 3σ bounds for the respective parameters.

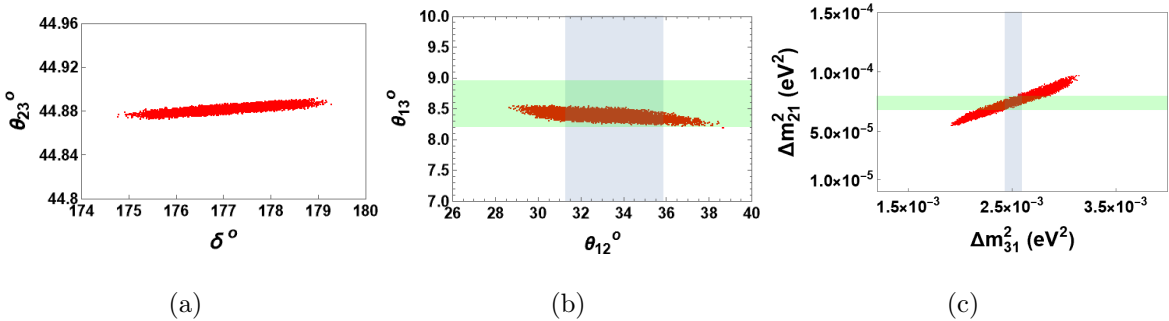


FIG. 3. The correlation plots between (a) θ_{23} and δ . (b) θ_{12} and θ_{13} . (c) Δm_{31}^2 and Δm_{21}^2 for normal ordering of neutrino masses. The blue and green strips represent the 3σ bounds for the respective parameters.

Parameters	Input values
m_3/eV	0.01-0.014
$\alpha/^\circ$	66.5-67.5
$\beta/^\circ$	47.5-48
$\phi_1/^\circ$	20-20.5
$\phi_2/^\circ$	80-80.5
$\phi_3/^\circ$	97-97.5

TABLE IV. Numerical values of the input parameters for texture M_ν^2 (Inverted Ordering)

Fields	D_{l_L}	l_R	ν_{l_R}	H	Φ	ζ	Δ
$SU(2)_L$	2	1	1	2	2	1	3
A_4	3	$(1, 1', 1'')$	$(1, 1', 1'')$	3	3	1	3
Z_3	1	$(\omega^2, \omega^2, \omega^2)$	(ω, ω, ω)	ω	ω^2	ω	1

TABLE V. The transformation properties of various fields under $SU(2)_L \times A_4 \times Z_3$.

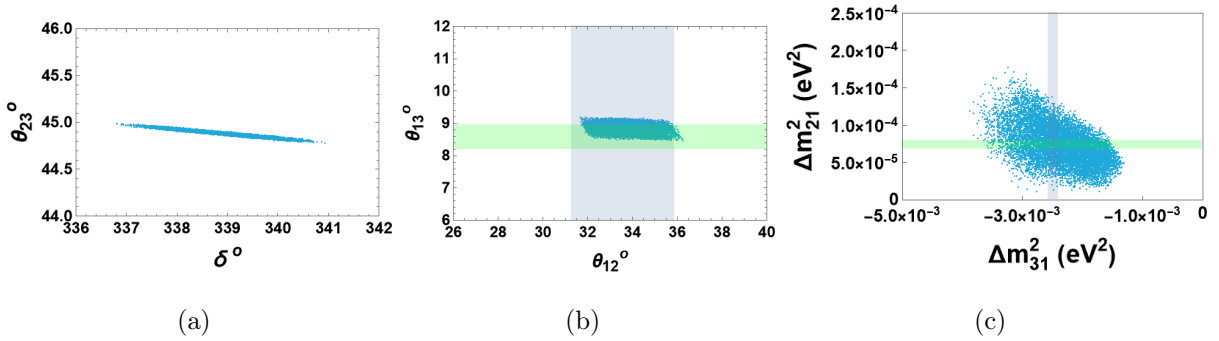


FIG. 4. The correlation plots between (a) θ_{23} and δ . (b) θ_{12} and θ_{13} . (c) Δm_{31}^2 and Δm_{21}^2 for inverted ordering of neutrino masses. The blue and green strips represent the 3σ bounds for the respective parameters.

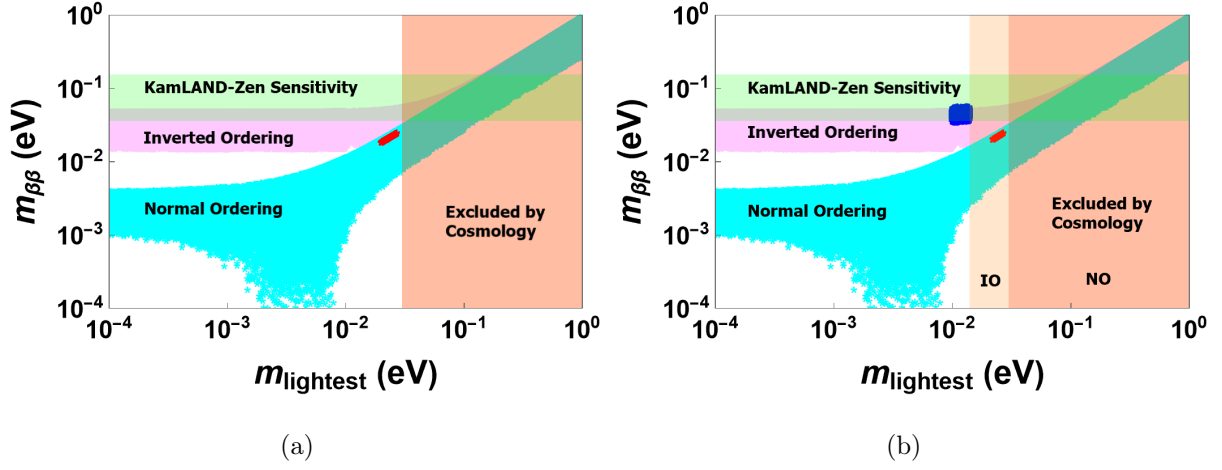


FIG. 5. (a) Shows the plot of effective Majorana neutrino mass $m_{\beta\beta}$ against the lightest neutrino mass for the texture M_ν^1 . (b) Presents the plot of effective Majorana neutrino mass $m_{\beta\beta}$ against the lightest neutrino mass for the texture M_ν^2 . The red and blue data points stand for normal and inverted orderings respectively.

Appendix B: The Scalar Potential

The $SU(2)_L \times A_4 \times Z_3$ invariant scalar potential can be constructed as shown in the following,

$$\begin{aligned}
 V = & V(H) + V(\Phi) + V(\Delta) + V(\zeta) + V(H, \Phi) + V(H, \Delta) + V(H, \zeta) + V(\Phi, \Delta) \\
 & + V(\Phi, \zeta) + V(\Delta, \zeta),
 \end{aligned} \tag{B1}$$

where,

$$\begin{aligned}
 V(H) = & \mu_H^2 (H^\dagger H) + \lambda_1^H (H^\dagger H)(H^\dagger H) + \lambda_2^H (H^\dagger H)_{1'} (H^\dagger H)_{1''} + \lambda_3^H (H^\dagger H)_{3_s} \\
 & (H^\dagger H)_{3_s} + \lambda_4^H (H^\dagger H)_{3_s} (H^\dagger H)_{3_a} + \lambda_5^H (H^\dagger H)_{3_a} (H^\dagger H)_{3_a},
 \end{aligned} \tag{B2}$$

$$\begin{aligned}
 V(\Phi) = & \mu_\Phi^2 (\Phi^\dagger \Phi) + \lambda_1^\Phi (\Phi^\dagger \Phi)(\Phi^\dagger \Phi) + \lambda_2^\Phi (\Phi^\dagger \Phi)_{1'} (\Phi^\dagger \Phi)_{1''} + \lambda_3^\Phi (\Phi^\dagger \Phi)_{3_s} (\Phi^\dagger \Phi)_{3_s} \\
 & + \lambda_4^\Phi (\Phi^\dagger \Phi)_{3_s} (\Phi^\dagger \Phi)_{3_a} + \lambda_5^\Phi (\Phi^\dagger \Phi)_{3_a} (\Phi^\dagger \Phi)_{3_a},
 \end{aligned} \tag{B3}$$

$$\begin{aligned}
V(\Delta) &= \mu_\Delta^2 Tr(\Delta^\dagger \Delta) + \lambda_1^\Delta Tr(\Delta^\dagger \Delta) Tr(\Delta^\dagger \Delta) + \lambda_2^\Delta Tr(\Delta^\dagger \Delta)_{1'} Tr(\Delta^\dagger \Delta)_{1''} \\
&\quad + \lambda_3^\Delta Tr(\Delta^\dagger \Delta)_{3_s} Tr(\Delta^\dagger \Delta)_{3_s} + \lambda_4^\Delta Tr(\Delta^\dagger \Delta)_{3_s} Tr(\Delta^\dagger \Delta)_{3_a} \\
&\quad + \lambda_5^\Delta Tr(\Delta^\dagger \Delta)_{3_a} Tr(\Delta^\dagger \Delta)_{3_a}, \tag{B4}
\end{aligned}$$

$$V(\zeta) = \mu_\zeta^2 (\zeta^\dagger \zeta) + \lambda^H (\zeta^\dagger \zeta) (\zeta^\dagger \zeta), \tag{B5}$$

$$\begin{aligned}
V(H, \Phi) &= \lambda_1^{H\Phi} (H^\dagger H) (\Phi^\dagger \Phi) + \lambda_2^{H\Phi} [(H^\dagger H)_{1'} (\Phi^\dagger \Phi)_{1''} + (H^\dagger H)_{1''} (\Phi^\dagger \Phi)_{1'}] \\
&\quad + \lambda_3^{H\Phi} (H^\dagger H)_{3_s} (\Phi^\dagger \Phi)_{3_s} + \lambda_4^{H\Phi} [(H^\dagger H)_{3_s} (\Phi^\dagger \Phi)_{3_a} + (H^\dagger H)_{3_a} (\Phi^\dagger \Phi)_{3_s}] \\
&\quad + \lambda_5^{H\Phi} (H^\dagger H)_{3_a} (\Phi^\dagger \Phi)_{3_a}, \tag{B6}
\end{aligned}$$

$$\begin{aligned}
V(H, \Delta) &= \lambda_1^{H\Delta} (H^\dagger H) Tr(\Delta^\dagger \Delta) + \lambda_2^{H\Delta} [(H^\dagger H)_{1'} Tr(\Delta^\dagger \Delta)_{1''} + (H^\dagger H)_{1''} Tr(\Delta^\dagger \Delta)_{1'}] \\
&\quad + \lambda_3^{H\Delta} (H^\dagger H)_{3_s} Tr(\Delta^\dagger \Delta)_{3_s} + \lambda_4^{H\Delta} [(H^\dagger H)_{3_s} Tr(\Delta^\dagger \Delta)_{3_a} + (H^\dagger H)_{3_a} \\
&\quad Tr(\Delta^\dagger \Delta)_{3_s}] + \lambda_5^{H\Delta} (H^\dagger H)_{3_a} Tr(\Delta^\dagger \Delta)_{3_a} + \mu_1 (H^T i \sigma_2 \Delta^\dagger H), \tag{B7}
\end{aligned}$$

$$V(H, \zeta) = \lambda_1^{H\zeta} (H^\dagger H) (\zeta^\dagger \zeta), \tag{B8}$$

$$\begin{aligned}
V(\Phi, \Delta) &= \lambda_1^{\Phi\Delta} (\Phi^\dagger \Phi) Tr(\Delta^\dagger \Delta) + \lambda_2^{\Phi\Delta} [(\Phi^\dagger \Phi)_{1'} Tr(\Delta^\dagger \Delta)_{1''} + (\Phi^\dagger \Phi)_{1''} Tr(\Delta^\dagger \Delta)_{1'}] \\
&\quad + \lambda_3^{\Phi\Delta} (\Phi^\dagger \Phi)_{3_s} Tr(\Delta^\dagger \Delta)_{3_s} + \lambda_4^{\Phi\Delta} [(\Phi^\dagger \Phi)_{3_s} Tr(\Delta^\dagger \Delta)_{3_a} + (\Phi^\dagger \Phi)_{3_a} \\
&\quad Tr(\Delta^\dagger \Delta)_{3_s}] + \lambda_5^{\Phi\Delta} (\Phi^\dagger \Phi)_{3_a} Tr(\Delta^\dagger \Delta)_{3_a}, \tag{B9}
\end{aligned}$$

$$V(\Phi, \zeta) = \lambda_1^{\Phi\zeta} (\Phi^\dagger \Phi) (\zeta^\dagger \zeta), \tag{B10}$$

$$V(\Delta, \zeta) = \lambda_1^{\Delta\zeta} Tr(\Delta^\dagger \Delta) (\zeta^\dagger \zeta), \tag{B11}$$

$$\tag{B12}$$

Based on the minimization of the scalar potential, the following equations hold good for the chosen vacuum expectation values (VEVs) $\langle H \rangle_\circ = v_H (1, 1, 1)^T$, $\langle \Phi \rangle_\circ = v_\Phi (1, 1, 1)^T$, $\langle \Delta \rangle_\circ = v_\Delta (0, 1, 0)^T$ and $\langle \zeta \rangle_\circ = v_\zeta$:

$$\begin{aligned}
\frac{dV}{dH_1} &= v_H (\mu_H^2 + (\lambda_1^{H\Delta} - \lambda_2^{H\Delta}) v_\Delta^2 + 2\mu_1 v_\Delta + \lambda_1^{H\zeta} v_\zeta^2 + (6\lambda_1^H + 8\lambda_3^H) \\
&\quad v_H^2 + 3\lambda_1^{\Phi H} v_\Phi^2 + 4\lambda_3^{\Phi H} v_\Phi^2) = 0, \tag{B13}
\end{aligned}$$

$$\begin{aligned}
\frac{dV}{dH_2} &= v_H (\mu_H^2 + (6\lambda_1^H + 8\lambda_3^H) v_H^2 + (\lambda_1^{H\Delta} + 2\lambda_2^{H\Delta}) v_\Delta^2 + \lambda_1^{H\zeta} v_\zeta^2 + 3\lambda_1^{\Phi H} v_\Phi^2 \\
&\quad + 4\lambda_3^{\Phi H} v_\Phi^2) = 0, \tag{B14}
\end{aligned}$$

$$\begin{aligned}
\frac{dV}{dH_3} &= v_H (\mu_H^2 + (6\lambda_1^H + 8\lambda_3^H) v_H^2 + (\lambda_1^{H\Delta} - \lambda_2^{H\Delta}) v_\Delta^2 + \lambda_1^{H\zeta} v_\zeta^2 + 3\lambda_1^{\Phi H} v_\Phi^2 \\
&\quad + 4\lambda_3^{\Phi H} v_\Phi^2) = 0, \tag{B15}
\end{aligned}$$

$$\begin{aligned} \frac{dV}{d\Phi_1} &= v_\Phi(3v_H^2\lambda_1^{\Phi H} + 4v_H^2\lambda_3^{\Phi H} + \mu_\Phi^2 + \lambda_1^{\Phi\Delta}v_\Delta^2 - \lambda_2^{\Phi\Delta}v_\Delta^2 + \lambda_1^{\Phi\zeta}v_\zeta^2 + 6\lambda_1^\Phi v_\Phi^2 \\ &\quad + 8\lambda_3^\Phi v_\Phi^2) = 0, \end{aligned} \quad (\text{B16})$$

$$\begin{aligned} \frac{dV}{d\Phi_2} &= v_\Phi(3v_H^2\lambda_1^{\Phi H} + 4v_H^2\lambda_3^{\Phi H} + \mu_\Phi^2 + \lambda_1^{\Phi\Delta}v_\Delta^2 + 2\lambda_2^{\Phi\Delta}v_\Delta^2 + \lambda_1^{\Phi\zeta}v_\zeta^2 + 6\lambda_1^\Phi v_\Phi^2 \\ &\quad + 8\lambda_3^\Phi v_\Phi^2) = 0, \end{aligned} \quad (\text{B17})$$

$$\begin{aligned} \frac{dV}{d\Phi_3} &= v_\Phi(3v_H^2\lambda_1^{\Phi H} + 4v_H^2\lambda_3^{\Phi H} + \mu_\Phi^2 + \lambda_1^{\Phi\Delta}v_\Delta^2 - \lambda_2^{\Phi\Delta}v_\Delta^2 + \lambda_1^{\Phi\zeta}v_\zeta^2 + 6\lambda_1^\Phi v_\Phi^2 \\ &\quad + 8\lambda_3^\Phi v_\Phi^2) = 0, \end{aligned} \quad (\text{B18})$$

$$\frac{dV}{d\Delta_1} = 2v_H^2((\lambda_3^{H\Delta} - \lambda_4^\Delta)v_\Delta + \mu_1) + 2(\lambda_3^{\Phi\Delta} - \lambda_4^{\Phi\Delta})v_\Delta v_\Phi^2 + 3v_1\lambda_1^{\Phi\Delta}v_\Phi^2 = 0, \quad (\text{B19})$$

$$\begin{aligned} \frac{dV}{d\Delta_2} &= v_\Phi^2(3\lambda_1^{H\Delta}v_\Delta + 2\mu_1) + v_\Delta(\mu_\Delta^2 + 3v_H^2\lambda_1^{\Phi\Delta} + (2\lambda_1^\Delta + i(\sqrt{3} + i)\lambda_2^\Delta)v_\Delta^2 \\ &\quad + \lambda_1^{\Delta\zeta}v_\zeta^2) = 0, \end{aligned} \quad (\text{B20})$$

$$\frac{dV}{d\Delta_3} = 2(v_H^2((\lambda_3^{H\Delta} + \lambda_4^{H\Delta})v_\Delta + \mu_1) + (\lambda_3^{\Phi\Delta} + \lambda_4^{\Phi\Delta})v_\Delta v_\Phi^2) = 0, \quad (\text{B21})$$

$$\frac{dV}{d\zeta} = 2v_\zeta(\mu_\zeta^2 + 3v_H^2\lambda_1^{H\zeta} + \lambda_1^{\Delta\zeta}v_\Delta^2 + 2\lambda^\zeta v_\zeta^2 + 3\lambda_1^{\Phi\zeta}v_\Phi^2) = 0. \quad (\text{B22})$$

In a similar way, the chosen VEVs $\langle H \rangle_\circ = v_H(1, 1, 1)^T$, $\langle \Phi \rangle_\circ = v_\Phi(1, 1, 1)^T$, $\langle \Delta \rangle_\circ = v_\Delta(\omega^2, 0, 1)^T$ and $\langle \zeta \rangle_\circ = v_\zeta$ can be justified based on the minimization conditions of the scalar potential.

Appendix C: Product Rules of A_4

The discrete group A_4 is a subgroup of $SU(3)$ which has 12 elements. The group has four irreducible representation out of which three are one dimensional and one three dimensional. In S-basis, the product of two triplets gives,

$$3 \times 3 = 1 + 1' + 1'' + 3_S + 3_A, \quad (\text{C1})$$

where,

$$1 = (a_1\bar{b}_1 + a_2\bar{b}_2 + a_3\bar{b}_3) \quad (\text{C2})$$

$$1' = (a_1\bar{b}_1 + \omega^2 a_2\bar{b}_2 + \omega a_3\bar{b}_3) \quad (\text{C3})$$

$$1'' = (a_1\bar{b}_1 + \omega a_2\bar{b}_2 + \omega^2 a_3\bar{b}_3) \quad (\text{C4})$$

$$(3 \times 3)_S = \begin{bmatrix} a_2 b_3 + a_3 b_2 \\ a_3 b_1 + a_1 b_3 \\ a_1 b_2 + a_2 b_1 \end{bmatrix}, \quad (\text{C5})$$

$$(3 \times 3)_A = \begin{bmatrix} a_2 b_3 - a_3 b_2 \\ a_3 b_1 - a_1 b_3 \\ a_1 b_2 - a_2 b_1 \end{bmatrix}. \quad (\text{C6})$$

The trivial singlet can be obtained from the following singlet product rules,

$$1 \times 1 = 1, \quad 1' \times 1'' = 1, \quad 1'' \times 1' = 1. \quad (\text{C7})$$